HIGH-TEMPERATURE OXIDATION OF SILICON CARBIDE COMPOSITES FOR NUCLEAR APPLICATIONS

M. STEINBRUECK, M. GROSSE, U. STEGMAIER

Karlsruhe Institute of Technology (KIT), Institute for Applied Materials (IAM-AWP)
Hermann-von Helmholtz-Platz 1, 76344 Eggenstein-Leopoldshafen – Germany

J. BRAUN, C. LORRETTE

Université Paris-Saclay, CEA, Service de Recherches Métallurgiques Appliquées
91 191 Gif-sur-Yvette Cedex – France

ABSTRACT

Three oxidation experiments at very high temperatures in steam atmosphere were conducted with advanced, nuclear grade SiC_f/SiC CMC cladding tube segments. One transient experiment was carried out until local failure of the sample at maximum temperature of approximately 1845°C. The failure was caused by complete consumption of the external CVD-SiC seal-coat resulting in steam access to the fibre-matrix composite with less corrosion resistance. Approaching these very high temperatures was accompanied by accelerated gas release mainly of H_2 and CO_2, formation of surface bubbles and white smoke. Two isothermal tests lasting 1 hour at 1700°C in steam with final flooding with water were run under nominally identical conditions. Both samples survived the tests without any macroscopic degradation. The mechanical performance of such quenched clad segments was not significantly affected with the maintenance of high capability to tolerate damages. Despite these harsh conditions of exposure, the SiC fibre-matrix load transfer remains efficient to provide ability to the composites to accommodate the deformation.

1. Introduction

Silicon carbide (SiC) ceramic matrix composites (CMC) are candidate materials for accident-tolerant fuel (ATF) cladding materials used in light water reactors (LWR) with the promise of highest survival temperature during severe accident scenarios. They offer excellent high-temperature mechanical properties, low density as well as high oxidation and irradiation resistances. As ceramic materials, however, they are the most revolutionary approach for new cladding tubes and other structural materials in nuclear reactors with a number of challenges that need to be addressed [1]. With this ambition, CEA (Commissariat à l'Energie Atomique et aux Energies Alternatives) makes systematic improvements of the original process to produce viable and robust nuclear grade SiC_f/SiC composites. SiC is the only binary solid compound in the Si-C system. More than 200 different crystal structures (polymorphs) are reported with the two major polytypes of silicon carbide being the metastable α-SiC having hexagonal crystal structure (similar to Wurtzite) and the thermodynamically stable β-SiC with a cubic zinc blende crystal structure (similar to diamond). The decomposition temperature is very high at around 2830°C. A vast number of papers has been published on silicon carbide and its behaviour at high temperatures; e.g. by Snead [2] and by Presser [3]. Reviews with special attention to the high-temperature oxidation behaviour of SiC were published e.g. by Narushima [4], Opila [5], and Roy [6].
Silica formed during oxidation of SiC also exists in several polymorphs - the amorphous phase and various crystalline phases. The crystalline phases are, from the low-temperature to the high-temperature, quartz, tridymite, and cristobalite, respectively. The melting temperature of SiO_2 is around 1700°C. The Pilling–Bedworth ratio, i.e. the ratio between the SiO_2 and the SiC substrate volumes, is approximately one, leading to a good bond at the interface with a very small stress build-up at the SiC/SiO_2 interface [2]. On the other hand, the thermal expansion coefficients of amorphous SiO_2 is lower than of SiC (and of β-cristobalite higher than of SiC [7]), which may lead to stresses in the silica scale during changes in temperature.

The oxidation of SiC in steam-containing atmospheres is complex compared e.g. to the oxidation of zirconium alloys. Its high-temperature resistance relies on the formation of a protective silicon oxide layer according to Equ. (1). Hydrogen is released in addition to carbon-containing gases. At higher temperatures, the formation of volatile hydroxides or oxyhydroxides may take place, e.g. according to Equ. (2) and Equ. (3). Furthermore, silicon monoxide, SiO, may be formed at low oxygen partial pressures and high temperatures. Formation and volatilisation of a silica layer at the same time finally lead to paralinear oxidation kinetics, as described by Equ. (4) with *X* being oxide thickness and *t* being time.

$$SiC + 3H_2O \rightarrow SiO_2 + CO + 3H_2 \quad (1)$$

$$SiO_2 + 2H_2O \rightarrow Si(OH)_4 \quad (2)$$

$$SiO_2 + H_2O \rightarrow SiO(OH)_2 \quad (3)$$

The parabolic growth rate of silica in steam in the absence of volatilization is around one order of magnitude faster than in dry oxygen atmosphere due to about 10 times larger permeability of H_2O and OH^- molecules in SiO_2 (100 times slower diffusion, but 1000 times greater solubility), according to Opila [8]. Based on the work published by Terrani [9], the correlation for the SiO_2 thickness during parabolic oxidation of SiC in steam is given in Equ. (5). The linear volatilization rate is strongly dependent on total pressure, steam partial pressure, and gas flow velocity. Corresponding relations were also published by Terrani [9].

$$\frac{dX}{dt} = \frac{k_p}{2X} - k_l \quad (4)$$

with X being oxide thickness, t time, k_p parabolic rate constant, and k_l linear rate constant.

$$k_p = 4.95 \cdot 10^{-5} \cdot \exp\left(\frac{-119000}{RT}\right) \left[\frac{m}{s^{0.5}}\right] \quad (5)$$

with R=8.314 J/mol·K and T in K.

Only a few literature sources deal with high-temperature oxidation of SiC-CMC cladding in steam. Without going into detail, Yueh and Terrani [10] tested CVD coated SiC_f/SiC specimens in steam between 1200°C and 1700°C. After 4 h of exposure at 1 atm pressure, no significant weight change was detected at 1200°C and 1600°C, and only a small weight loss was detected at 1700°C. Terrani [9] published results of steam oxidation of various SiC samples between 1200°C and 1700°C and varying pressure between 0.1 and 2 MPa. Identical oxidation behaviour was found between monolithic CVD SiC and CVD coated SiC fibres composites, as long as the environmental barrier coating (EBC) remained intact. On the other hand, non-coated SiC_f/SiC composite was strongly degraded. Steam oxidation of CVD SiC up to 1700°C resulted in uniform materials recession with slow kinetics (< 1 mg/cm²/h). Steam oxidation as a function of its partial pressure of different SiC CMC samples up to 2000°C including final quenching by water was investigated by Avincola [11]. For the lower steam partial pressures (10-30kPa), the parabolic constants (k_p) were in agreement with the data from literature obtained at lower temperatures. At 1600°C and 60 kPa, the mass gain became irregular due to the formation of bubbles, which increased with exposure time and steam partial pressure. Despite bubble formation, all samples remained intact with only minor superficial degradation. Furthermore, 1-hour oxidation tests at 1700°C and 1800°C resulted in silica layers of around 2 µm. Most of the samples oxidised in steam during ramp tests from 1400°C to 2000°C (10 K/min) even withstood quenching from 2000°C [11].

The formation of bubbles in the silica scale was observed by several authors [8] [9] [12] [13], showing increasing tendency for bubble formation along with increasing temperature and steam partial pressure.

This paper will present and discuss results of oxidation experiments up to 1850°C with SiC_f/SiC CMC cladding segments manufactured by CEA. The experiments were conducted at KIT; post-test examinations were performed in both institutes.

2. Experimental conditions

2.1. Samples

Three 6-cm-long SiC_f/SiC samples were manufactured by CEA. The composite materials consist of CVI-SiC_f/SiC tubes processed in the standard LWR nuclear fuel assembly geometry. Third generation Hi-Nicalon type S fibres (NGS Advanced Fibers Co., LTD) were employed as reinforcement. Two successive fibres layers at ±45° were applied by filament winding to confer the material mechanical performances. The SiC matrix was chemically infiltrated by CVI process after deposition of a thin pyrocarbon interphase (50 – 100 nm). The inner and outer CVD SiC surfaces were then ground to meet to dimension requirements. The final porosity volume fraction is below 10%. More details about the manufacturing process can be found in [14]. The samples are filled with graphite (used as a susceptor for the high-frequency (HF) inductive heating purpose [11]) and tightly sealed with end caps at both sides (Fig. 1).

2.2. Test facility and conduct

The experiments were conducted in the QUENCH-SR (single rod) facility with inductive heating and the possibility of quenching of the samples by water. The samples are enclosed in a quartz glass tube allowing observation of the test by video recording. A water-cooled copper coil surrounding the glass tube generates a magnetic field inducing eddy currents in the metallic sample, Fig. 1. Power is provided by a HF generator with a power of 20 kW working at a frequency up to 700 kHz. Temperature is measured and controlled via a two-colour pyrometer (type IGAR 12-LO MB22) with a measuring range of 500 to 2200°C working at the wavelengths 1.28 µm and 1.65 µm.
Gas supply is controlled by a Bronkhorst® gas flow controller, water flow controller and a CEM (controlled evaporator and mixer). 40 L/h argon flow through the facility throughout all tests, and 60 g/h steam was injected during the oxidation phases resulting in a steam concentration of 65 vol.%. The off-gas line is connected to a mass spectrometer (MS, IPI GAM 3000) for quantitative measurement of H_2O, H_2, CO, CO_2, CH_4 and other gases with Ar as reference. The MS was calibrated for all relevant gases before the tests.
The transient test (SiC-01) was conducted from 600°C until failure of the sample with steam switched on at 1400°C. The heating rate was 10 K/min during the whole test. The test was terminated by switching off power and the steam flow after first indication of strong degradation, i.e. local hot spot, high concentrations of reaction gases and fume production. Hence, the sample quickly cooled down in a humid argon flow without quenching.
Two identical isothermal tests (SiC-02 and SiC-03) were conducted for one hour at 1700°C. The samples were heated from 600°C to 1700°C with a rate of 1 K/s in argon. Steam flow was switched on approximately 90 s after reaching the isothermal plateau. The tests were terminated by quenching with a rising cylinder filled with water at 95°C at a quench rate of approximately 1 cm/s. The power supply was switched off when the water level reached the lower end of the sample.
All tests were video recorded during the oxidation phases in steam as shown in Fig. 1.

2.3. Post-test examinations

The mass of the samples was measured before and after tests. The pre- and post-test appearance was documented non-destructively by photography (Canon EOS 1200D), SEM/EDS (FEI XL30S with Silicon Drift Detector EDS detector), and X-ray tomography (Inspection Technologies v/tome/x-s).
The ramp-tested (SiC-01) and one isothermally tested (SiC-03) samples were cut longitudinally, embedded in epoxy resin, ground and polished for ceramographic analyses of the cross sections.
A uniaxial tensile test was performed at room temperature on the second isothermally oxidized sample (SiC-02) to assess the residual mechanical behaviour and performances. The mechanical test was carried out up to failure in accordance with ISO 20323 standard, followed by a SEM analysis of the fracture surfaces.

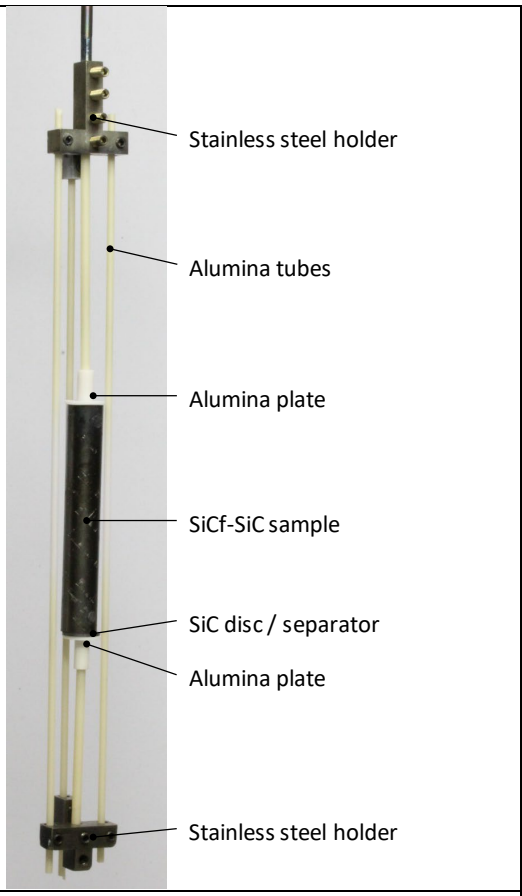

Sample holder

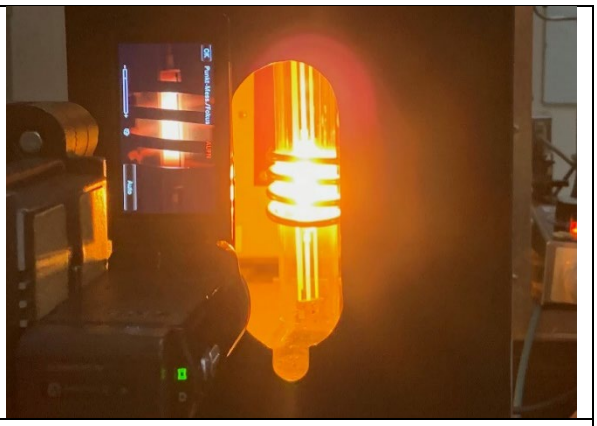

QUENCH-SR with sample and video recording at approximately 1800°C

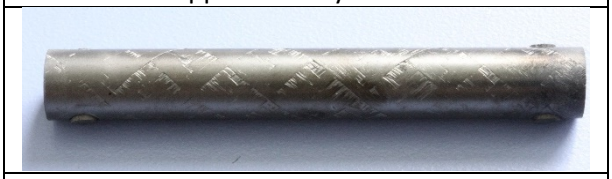

SiC_f/SiC sample before test

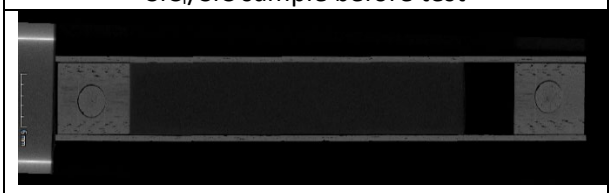

SiC_f-SiC sample before test (tomography)

Fig. 1: QUENCH-SR facility and SiC_f-SiC sample

3. Experimental results and discussion

3.1. Transient test until failure

The experiments went without any specific issue; the heating via the graphite core and the control of temperature by pyrometer worked well. The temperature history and the main results of the MS measurements for the SiC-01 test are summarized in Fig. 2.

The oxidation rate was in-situ measured by the gas concentrations and converted into release rates using the Ar flow rate as reference. The releases of hydrogen and CO_2, and to a lesser extent of CO, were immediately measured after start of the steam injection above 1400°C. A very low signal of methane, CH_4, appeared throughout the test. H_2 and CO_2 release rates increased up to 1490°C and then remained more or less constant up to 1730°C. From 1730 to 1820°C, a linear increase of gas release rates was observed before a strong oxidation escalation resulted in a fast increase of gas release rates up to termination of the test. Interestingly, the CO release rate only increased beyond 1820°C.

First bubbles at the sample surface were observed at 1820°C; first visual indication of smoke formation was at 1840°C. The test was stopped by switching off power and steam injection after stronger development of smoke in the test section at the maximum temperature of 1845°C. Fig. 3 provides some snapshots taken from the video approaching the end of the experiment. They show formation of bubbles (3rd and 4th image) and smoke (5th image).

Some pieces of spalled-off SiC layers and produced SiO_2 were found at the bottom of the test rig after the test contributing to a mass loss of the sample of 50.5 mg, corresponding to 0.36 wt%.

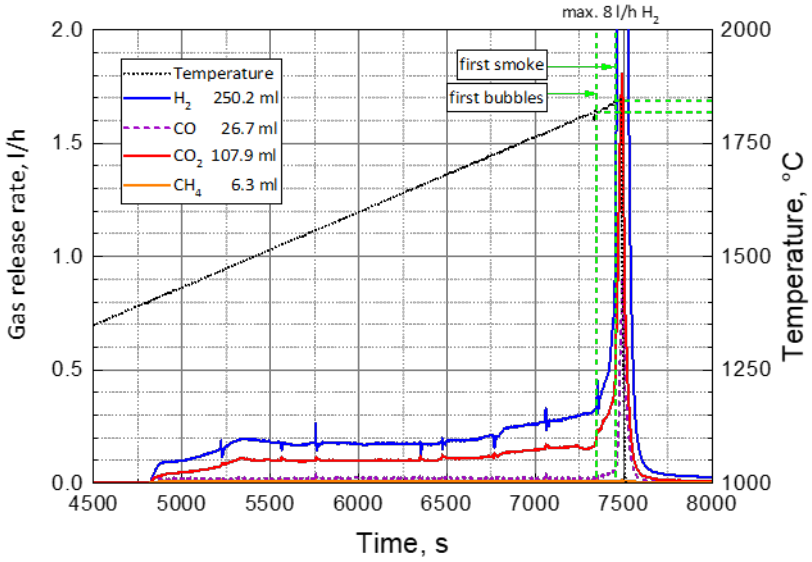

Fig. 2: Temperature history and gas release rates during transient test SiC-01. The numbers in the legend correspond to the integral values of gas release.

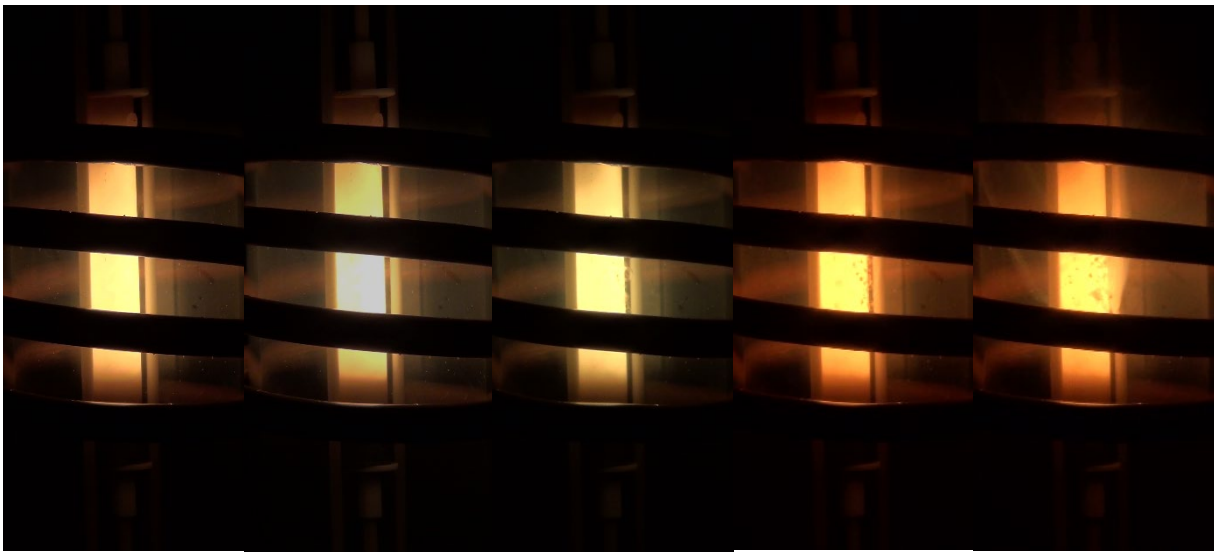

6698 s, 1716°C 7298 s, 1816°C 7408 s, 1835°C 7438 s, 1840°C 7483s, 1845°C

Fig. 3: Video snapshots taken at the times and temperatures given during transient test SiC-01

Post-test examinations

The sample is locally degraded as it can be seen in Fig. 4, but remained intact, i.e. did not break and kept its geometry. No sign of through-wall degradation and corresponding steam attack of graphite was seen by X-ray tomography and later on by ceramography.

Locally, the external CVD SiC layer was consumed/removed, resulting in the high gas release rates as shown in Fig. 2. Fig. 5 provides optical micrographs of the longitudinal cross section at and below the failure position. It is clearly seen that the fibres are exposed in the damage region and having interacted with the steam atmosphere. At lower and higher positions of the sample (with lower temperatures), the external CVD layer remained intact. In those areas, a 2-3 µm thick silica scale was measured by SEM/EDX.

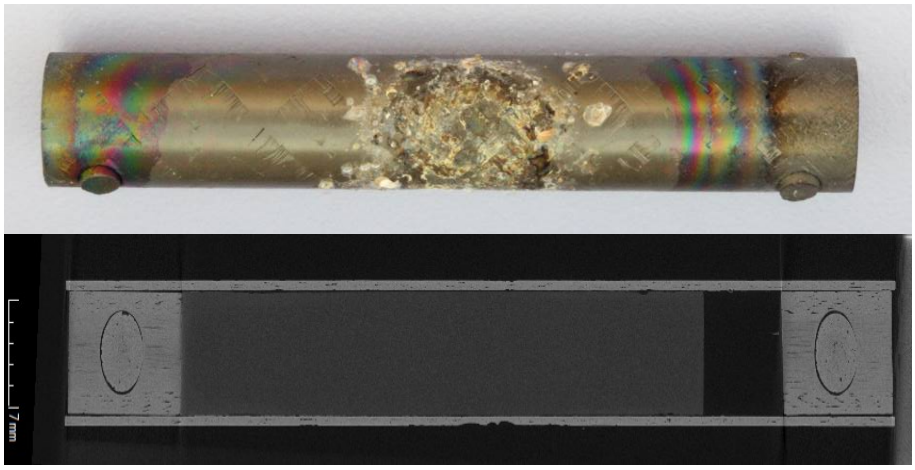

Fig. 4: Post-test appearance of the sample after the transient test up to 1845°C (top) and X-ray tomography longitudinal cut (bottom)

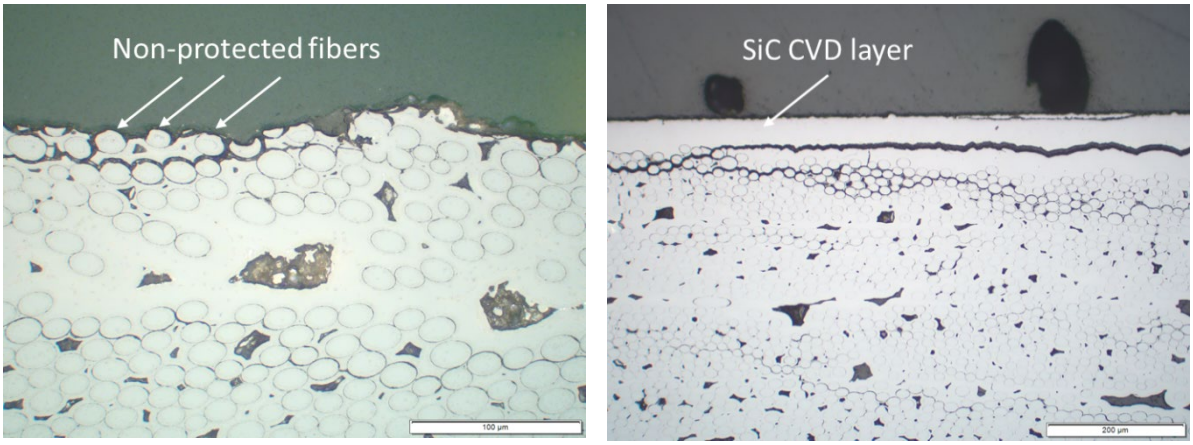

Fig. 5: Optical micrographs from the failure region in the middle of the sample (left) and from the non-failure region below (right)

3.2. Isothermal tests at 1700°C

Both tests ran under nominally the same conditions without technical problems during all test phases. The visual observation during the tests (also video recorded) showed slight irregularities at the surface of sample SiC-02, including dark dots, which could be caused by the formation of small bubbles. The formation of one big bubble was seen in test SiC-03 after approximately 16 min in the steam phase, which reached its maximum size 4 min later and remained stable for approximately 30 min.

Gas release rates of relevant gases (H_2, CO_2, CO, and CH_4) are presented in Fig. 6. The release rates are slightly higher for the SiC-02 sample, which is also reflected by the figures for the integral release of the gases as shown in the diagrams legends. The detailed trend of the gas flow curves is very similar for both tests, with an initial (simultaneous to steam injection) sharp increase for all gases, followed by a slight reduction and increase again for hydrogen and carbon dioxide. The CO curve follows a somehow opposite behaviour in that phase. All release rates of the produced gases sharply increase with initiation of the quench process; but these data have to be treated with caution because of the very low concentration of the reference gas argon in this phase.

The mass change of the samples was -0.67 wt% and -0.49 wt% for SiC-02 and SiC-03, respectively.

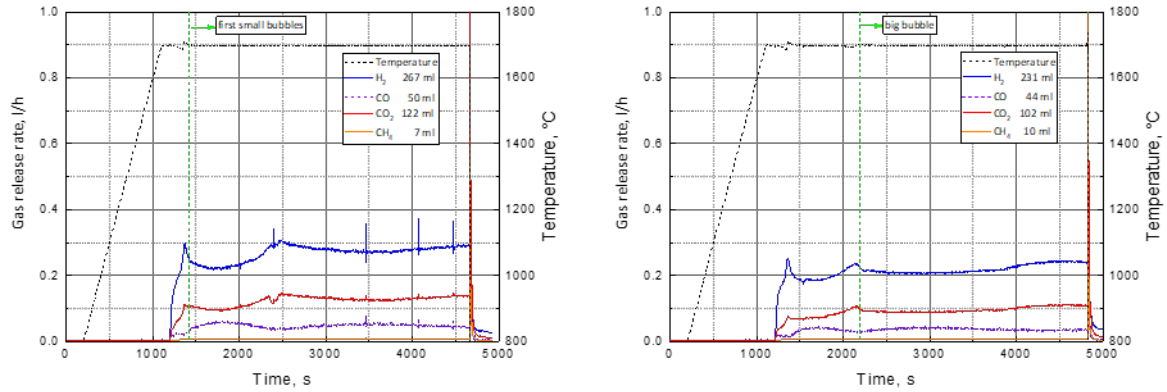

Fig. 6: Temperature history and gas release rates of the isothermal tests SiC-02 (left) and SiC-03 (right)

Post-test examinations

The post-test appearance of the samples is very similar (Fig. 7). The surface appears stained and tempering colours are seen at the ends of the tube segments. The latter result from the temperature gradient toward the ends of the samples (without graphite susceptor) and indicate thin silica scales with changing thickness in the order of magnitude of the light wavelengths.

Fig. 7: Post-test appearance of the samples after 1 h isothermal oxidation in steam at 1700°C

X-ray tomography showed no degradation of the SiC tube segments, neither externally from the interaction with steam nor internally due to interaction with the graphite susceptor. Two representative SEM images of each sample are provided in Fig. 8. The top view images in the upper row show small silica bubbles, burst for SiC-02 and closed for SiC-03. The lower images show higher magnified side views of the surfaces with similar appearance, but also open bubbles for SiC-03. The images were taken at different positions of the samples. EDX analyses of the samples surfaces showed only SiO_2.

The two images in Fig. 9 show micrographs of sample SiC-03 obtained by optical microscopy and SEM. As expected from the online and tomography results, the CVD-SiC seal-coat remained intact during the 1-hour oxidation at 1700°C. Furthermore, no indications of interaction between SiC and graphite (susceptor) was found. The SiO_2 scale produced by the oxidation of SiC was around 1 µm thick with single measurement values between 0.5 and 1.6 µm. Regarding the overall mass loss of the sample, it could be assumed that this oxide scale thickness corresponds to the equilibrium value of the paralinear oxidation determined by growth and volatilization of SiO_2 [15]. Furthermore, the oxide thickness measured on this sample well corresponds to other data published for oxidation of SiC in steam at 1700°C [9] [11] [13].

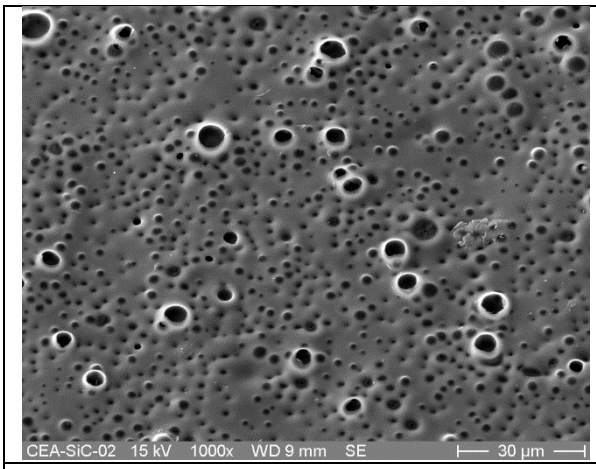

SiC-02 surface 1000x top view

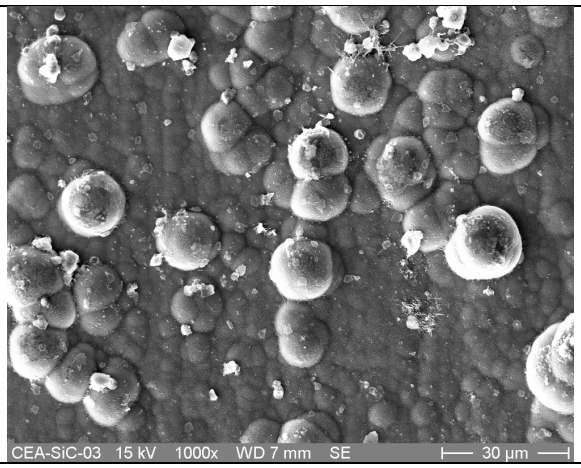

SiC-03 surface 1000x top view

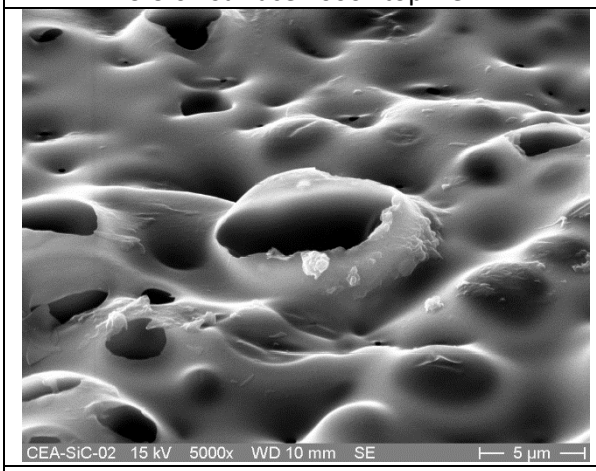

SiC-02 surface 5000x side view

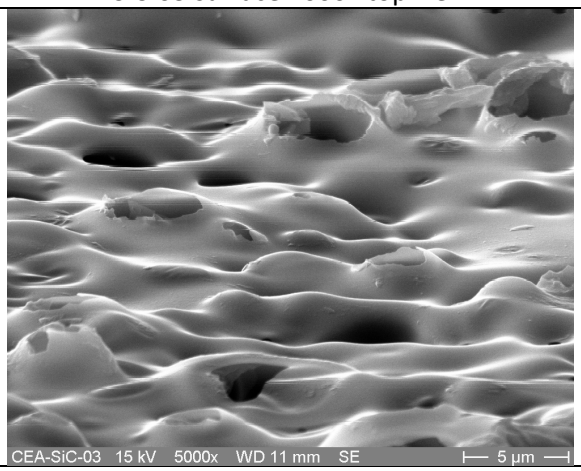

SiC-03 surface 5000x side view

Fig. 8: SEM images of both samples SiC-02 & SiC-03 surfaces after 1 h isothermal oxidation in steam at 1700°C

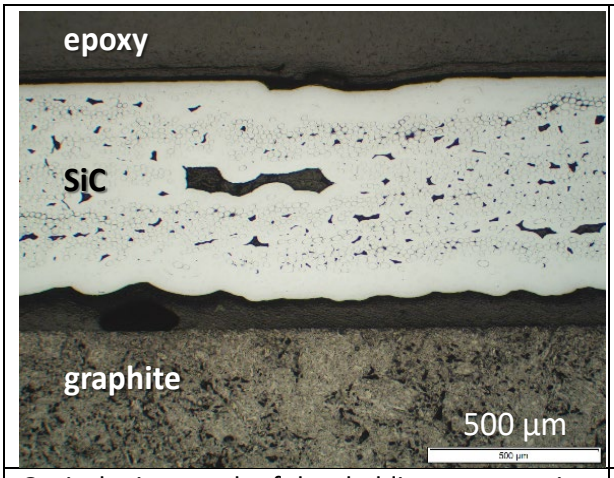

Optical micrograph of the cladding cross section

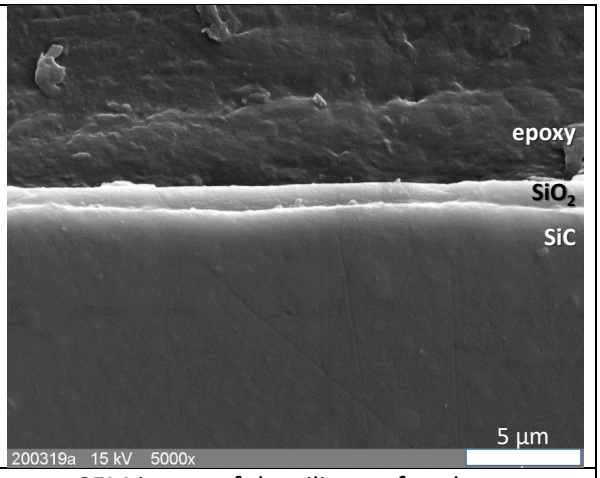

SEM image of the silica surface layer

Fig. 9: Cross section micrographs of sample SiC-03 after 1 h oxidation in steam at 1700°C

Mechanical testing

Figure 10 reports the residual stress-strain curves measured under tensile monotonic loading on the SiC-02 sample after oxidation with the monitoring of the acoustic emission. Undoubtedly, the oxidation conditions affect the mechanical behaviour with a slight decrease of the mechanical properties in

comparison to reference values measured on the pristine material (see Table 1). However, a non-linear elastic failure behaviour with a plateau resulting of the matrix micro-cracking is maintained. This is the consequence of low interfacial shear strength due to the presence of the pyrocarbon interphase, which does not seem to be affected. Despite the harsh conditions of exposure, the fibre-matrix load transfer remains efficient to provide ability to the composites to accommodate the deformation.

SEM post-examination of the fracture surfaces largely exhibit predominant non-brittle areas that are characterized by non-oxidized fibre pull out with high lengths. A distinction is made between the inner and outer sides and possibly due to the specificity of the oxidizing flux in the furnace. In any case, the overall oxidation kinetics of the external silicon carbide produce a protective silica layer on the surface without clear evidences of any local penetration.

The mechanical properties loss is attributed to the tensile strength decrease of the Hi-Nicalon type S fibres coming from the thermal treatment [16]. Indeed, the authors have already shown that the fibres keep their mechanical properties up to 1600°C, but lose their mechanical strength between 1600 and 1780°C. Therefore, it is very likely that the 1700°C thermal treatment is responsible for the degradation of the mechanical properties.

Finally, the thermal shock due to the water quenching does not seem to have significant impact on the mechanical responses, which is consistent with previous results. Whether the CVI-SiC/SiC specimen were quenched or not, only a single regime of acoustic emission was detected indicating that matrix cracking saturation did not occur up to the ultimate failure [17].

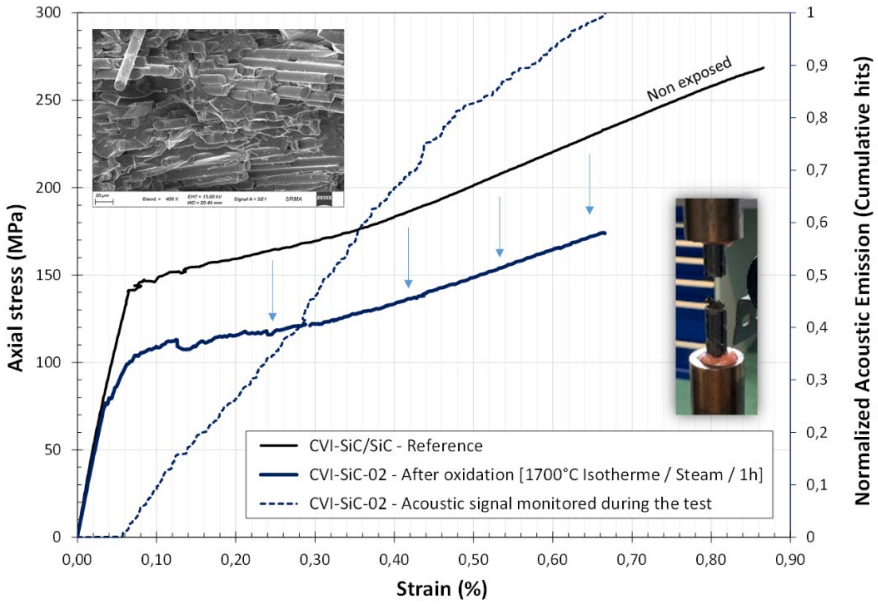

Fig. 10: Uniaxial tensile stress-strain behaviour measured on sample SiC-02 at ambient temperature after 1 h isothermal oxidation in steam at 1700°C. The reference stress-strain curve measured on the pristine material is given for comparison. A representative area of the fracture surface is given in the inset.

Tab 1. Residual uniaxial tensile properties measured after 1h isothermal oxidation at 1700°C in steam followed by water quenching. Reference data of the pristine material are also reported.

Sample	Young modulus EP (GPa)	Yield strength σ_y (MPa)	Strain ε_y (%)	Tensile strength σ_m (MPa)	Strain at failure ε_m (%)
SiC-02 1h 1700°C steam final quenching	227	92	0.056	174	0.66
SiC_f/SiC reference average of 3 samples	260 ± 7	107 ± 15	0.048 ± 0.012	274 ± 6	0.90 ± 0.05

4. Summary and conclusions

Three oxidation experiments at very high temperatures in steam atmosphere were conducted with advanced nuclear grade SiC_f/SiC CMC cladding tube segments. The samples were heated internally by HF induction of a cylindrical graphite susceptor without chemical interaction evidenced between the SiC cladding and the graphite susceptor.

One transient experiment was carried out until local failure of the sample at maximum temperature of approximately 1845°C. The failure was caused by complete consumption of the external CVD-SiC seal-coat resulting in steam access to the fibre-matrix composite with enhanced oxidation kinetics. Approaching these very high temperatures was accompanied by accelerated gas release mainly of H_2 and CO_2, formation of surface bubbles and white smoke. The smoke presumably consisted of volatile and in colder areas condensing Si-O-H species like SiO and $Si(OH)_4$.

Two isothermal tests for one hour at 1700°C in steam with final quenching by water were run under identical conditions. Both samples survived the tests without any macroscopic degradation. The SiC seal-coat remained intact and avoided attack of the SiC fibres by steam. The gas release rates as an indicator for the oxidation rate remained low and roughly constant throughout the tests. Quenching by 95°C water resulted in no visible macroscopic cracks or spallation. Even though a slight decrease in mechanical performances of around 15% is observed, the SiC_f/SiC composite retains its beneficial damage-tolerant behaviour after exposure in such harsh oxidizing conditions. This decrease in the mechanical properties is probably due to the fibres' strength loss with ageing during annealing at very high temperatures; but further investigations need to be conducted to verify this assumption.

These positive results enable identifying the maximal temperature that can be withstood by advanced nuclear SiC-based fuel cladding material to face accidental situations in LWR. They confirm excellent oxidation resistance up to 1700°C and give first indications on the degradation mechanisms that operate beyond this temperature level.

5. Acknowledgements

The authors thank P. Severloh (KIT) for ceramographical examination of the samples, A. Meier (KIT) for the X-ray tomography investigation and E. Rouesne (CEA) for the SEM fracture surfaces observation.
This research has received funding from the Euratom Research and Training Programme 2014–2018 under grant agreement No. 740415 (H2020 IL TROVATORE).

6. References

[1] K. Terrani, "Accident tolerant fuel cladding development: Promise, status, and challenges," *Journal of Nuclear Materials,* vol. 501, pp. 13-30, 2018.

[2] L. Snead, T. Nozawa, Y. Katoh, T.-S. Byun, S. Kondo and D. Petti, "Handbook of SiC properties for fuel performance modeling," *Journal of Nuclear Materials,* vol. 371, pp. 329-377, 2007.

[3] V. Presser and K. Nickel, "Silica on Silicon Carbide," *Critical Reviews in Solid State and Materials Sciences,* vol. 33, pp. 1-99, 2008.

[4] T. Narushima, T. Goto, T. Hirai and Y. Iguchi, "High-Temperature Oxidation of Silicon Carbide and Silicon Nitride," *Materials Transactions, JIM,* vol. 38, pp. 821-835, 1997.

[5] E. Opila and N. Jacobson, "Oxidation and Corrosion of Ceramics," in *Ceramics Science and Technology*, Wiley, 2013.

[6] J. Roy, S. Chandra, S. Das and S. Maitra, "Oxidation behaviour of silicon carbide - A review," *Reviews on Advanced Materials Science,* vol. 38, pp. 29-39, 2014.

[7] F. Cao, W. Hao, X. Wang, F. Guo, X. Zhao, N. Rohbeck and P. Xiao, "Effects of water vapor on the oxidation and the fracture strength of SiC layer in TRISO fuel particles," *Journal of the American Ceramic Society,* vol. 100, pp. 2154-2165, 2017.

[8] E. Opila, “Variation of the Oxidation Rate of Silicon Carbide with Water-Vapor Pressure,” *Journal of the American Ceramic Society,* vol. 82, pp. 625-636, 1999.

[9] K. Terrani, B. Pint, C. Parish, C. Silva, L. Snead and Y. Katoh, “Silicon carbide oxidation in steam up to 2 MPa,” *Journal of the American Ceramic Society,* vol. 97, pp. 2331-2352, 2014.

[10] K. Yueh and K. Terrani, “Silicon carbide composite for light water reactor fuel assembly applications,” *Journal of Nuclear Materials,* vol. 448, pp. 380-388, 2014.

[11] V. Angelici Avincola, M. Grosse, U. Stegmaier, M. Steinbrueck and H. Seifert, “Oxidation at high temperatures in steam atmosphere and quench of silicon carbide composites for nuclear application,” *Nuclear Engineering and Design,* vol. 295, p. 468–478, 2015.

[12] B. Schneider, A. Guette, R. Naslain, M. Cataldi and A. Costecalde, “A theoretical and experimental approach to the active-to-passive transition in the oxidation of silicon carbide: Experiments at high temperatures and low total pressures,” *Journal of Materials Science,* vol. 33, pp. 535-547, 1998.

[13] H. Pham, Y. Nagae, M. Kurata, D. Bottomley and K. Furumoto, “Oxidation kinetics of silicon carbide in steam at temperature range of 1400 to 1800 °C studied by laser heating,” *Journal of Nuclear Materials,* vol. 529, p. art. no. 151939, 2020.

[14] J. Braun, C. Sauder, J. Lamon and F. Balbaud-Célérier, "Influence of an original manufacturing process on the properties and microstructure of SiC/SiC tubular composites," *Composites Part A: Applied Science and Manufacturing,* vol. 123, pp. 170-179, 2019.

[15] S. Rashkeev, M. Glazoff and A. Tokuhiro, “Ultra-high temperature steam corrosion of complex silicates for nuclear applications: A computational study,” *Journal of Nuclear Materials,* vol. 444, pp. 56-64, 2014.

[16] J. Sha, T. Nozawa, J. Park, Y. Katoh and A. Kohyama, “Effect of heat treatment on the tensile strength and creep resistance of advanced SiC fibers,” *Journal of Nuclear Materials,* Vols. 329-333, pp. 592-596, 2004.

[17] C. G. T. Lorrette, F. Bourlet, C. Sauder, L. Briottet, H. Palancher, J. Bischoff and E. Pouillier, “Quench behavior of SiC/SiC cladding after a high temperature ramp under steam conditions,” in *Water Reactor Fuel Performance Meeting*, Jeju-do, South Korea, 2017.